Am J Cancer Res 2021;11(4):1148-1169
www.ajcr.us /ISSN:2156-6976/ajcr0125917

Original Article

Cilostazol eliminates radiation-resistant glioblastoma by re-evoking big conductance calcium-activated potassium channel activity

Chan-Chuan Liu[1], Cheng-Lin Wu[3], I-Chun Yeh[6], Sheng-Nan Wu[2], Chun-I Sze[1,3*], Po-Wu Gean[1,4,5*]

[1]Institute of Basic Medical Sciences, [2]Department of Physiology, [3]Department of Pathology, National Cheng Kung University Hospital, Taiwan; [4]Department of Pharmacology, College of Medicine, National Cheng-Kung University, Tainan, Taiwan; [5]Department of Biotechnology and Bioindustry Sciences, National Cheng-Kung University, Tainan, Taiwan; [6]Department of Radiation Oncology, Kuo General Hospital, Tainan, Taiwan. [*]Equal contributors.

Received November 9, 2020; Accepted February 4, 2021; Epub April 15, 2021; Published April 30, 2021

Abstract: In spite of radio- and chemotherapy, glioblastoma (GBM) develops therapeutic resistance leading to recurrence and poor prognosis. Therefore, understanding the underlying mechanisms of resistance is important to improve the treatment of GBM. To this end, we developed a radiation-resistant cell model by exposure to consecutive periods of irradiation. Simultaneously, single high-dose irradiation was introduced to determine "when" GBM developed consecutive irradiation-induced resistance (CIIR). We found that CIIR promoted TGF-β secretion, activated pro-survival Akt, and downregulated p21 in a p53-independent manner. Furthermore, CIIR upregulated multidrug-resistant proteins, resulting in temozolomide resistance. CIIR GBM also enhanced cell mobility and accelerated cell proliferation. The big-conductance calcium-activated potassium channel (BK channel) is highly expressed and activated in GBM. However, CIIR diminishes BK channel activity in an expression-independent manner. Cilostazol is a phosphodiesterase-3 inhibitor for the treatment of intermittent claudication and was able to reverse CIIR-induced BK channel inactivation. Paxilline, a BK channel blocker, promoted cell migration and proliferation in parental GBM cells. In contrast, Cilostazol inhibited CIIR-induced cell motility, proliferation, and the ability to form tumor spheres. Moreover, we established a radiation-resistant GBM *in vivo* model by intracranially injecting CIIR GBM cells into the brains of NOD/SCID mice. We found that Cilostazol delayed tumor *in vivo* growth and prolonged survival. As such, inactivation of the BK channel assists GBM in developing radiation resistance. Accordingly, restoring BK channel activity may be an effective strategy to improve therapeutic efficacy, and cilostazol could be repurposed to treat GBM.

Keywords: Glioblastoma, radiation resistance, big conductance calcium-activated potassium channel, Cilostazol

Introduction

Glioblastoma (GBM) is the most aggressive primary brain tumor. The current standard of treatment consists of gross total surgical removal of the tumor mass with adjuvant radiation therapy alone, chemotherapy alone, or combined radiochemotherapy [1]. The World Health Organization reported that the post-treatment median survival of GBM patients is 15-18 months [2, 3]. Although radiation is a powerful approach in local tumor control, which can significantly improve patient survival, the benefit of radiochemotherapy is marginal [4, 5]. Mechanistically, radiation not only leads to cell death, but activates intrinsic anti-death and pro-survival mediators in the residual cancer cells [4, 6, 7]. However, the complexity of cellular responses to irradiation enhances radiation-induced malignancy, such as cell proliferation, migration, and invasion [8]. As such, radiation resistance is a critical indicator to explain why treatment fails and cancers recur [9].

Calcium-activated potassium channels are abundantly expressed and activated in GBM [10]. These channels modulate potassium current to regulate a variety of cell behaviors pertinent to morphology and consist of three kinds of potassium channels, namely big-conductance (BK), intermediate-conductance (IK), and small-conductance (SK) channels [11-13]. Calcium-

activated potassium channels also regulate radiation response in cancers, such as activation or up-regulation of IK and BK channels promoting cell migration after radiation therapy [6, 14, 15].

However, little is known about how calcium-activated potassium channels contribute to the development of radiation resistance in GBM. Therefore, we mimicked the radiotherapy procedure and modified Yan's method to develop radiation-resistant GBM *in vitro* and *in vivo* [16]. The influences of consecutive periods of irradiation on calcium-activated potassium channels were investigated. In addition, Cilostazol, a selective phosphodiesterase-3 inhibitor, is used for the treatment of intermittent claudication. A previous study reported that Cilostazol is able to specifically activate BK channels by directly binding to them without the presence of cytoplasmic factors [17]. In the present study, we investigated the role of calcium-activated potassium channels in radiation resistance and the therapeutic potential of Cilostazol for radiation-resistant GBM assessed in both *in vitro* and *in vivo* models.

Material and methods

Cell culture

The human glioblastoma (GBM) cell line 1306MG was obtained from Dr. Carol A. Kruse, a professor of Department of Neurosurgery, UCLA Medical Center, US, while the human GBM cell line U87MG was obtained from Dr. Shur-Tzu Chen, a professor of Department of Cell Biology and Anatomy, NCKU, Taiwan. The GBM cells were maintained in Dulbecco's Modified Eagle Medium (DMEM, Simply) with 10% fetal bovine serum (FBS, Gibco), penicillin (100 U/ml)/streptomycin (100 μg/ml) (Simply), and 50 μg/ml gentamycin (Thermo). Cells were incubated under a humidified atmosphere of 5% CO_2 at 37°C.

Developing radiation-resistant glioblastoma cell lines

GBM cells were subjected to γ-ray irradiation by a clinical-use accelerator in the Department of Radiation Oncology of Kuo General Hospital in Tainan, Taiwan, with a radiation dose ranging from 2 to 10 Gy. At 24 hours post-irradiation, the cells were suspended, and the relative living cell number was calculated by performing Trypan blue exclusion assay. Cell viability was analyzed by Microsoft Excel 2013. In order to establish radiation-resistant human GBM cell lines, the median effective dose of irradiation was selected to develop consecutive irradiation-induced resistance. The cell viability of a single high dose of irradiation was used as the positive control. When the viability of the GBM cells under consecutive irradiation was higher than that of a single high dose of irradiation, the GBM cell line was defined as radiation-resistant.

Western blotting

The cells were collected and lysed in a buffer containing 20 mM Tris, 150 mM Sodium Chloride, 1 mM EDTA, 1 mM EGTA, 1% Triton X-100, 2.5 mM Sodium Pyrophosphate, 1 mM 2-Glycerophosphate, 1 mM Sodium Orthovanadate, and 1 tab/100 ml Protease inhibitor (Roche). The protein expression was evaluated by semi-quantitative Western blotting. Rabbit anti-rabbit pAkt (Ser473), rabbit anti-Akt, rabbit anti-p21, rabbit anti-pp53 (Cell Signaling Technology), mouse anti-BKβ, mouse anti-GAPDH, goat anti-p53, mouse anti-ABCG2, mouse anti-MRP5 (Santa cruz), rabbit anti-BK channel, and mouse anti-β-actin (Sigma) were used along with horseradish peroxidase-conjugated secondary antibody (Jackson ImmunoResearch). The band intensities were quantified by a BioSpectrum® Imaging System.

Enzyme-linked immunosorbent assay (ELISA)

At 24 hours post-cell seeding, the cultured medium was refreshed. After culturing for 48 hours, the cultured medium was collected. The condition medium was separated from the insoluble material by centrifugation (5000 × g, 10 min, 4°C). The total TGF-β1 concentration was then measured by standard ELISA protocol (Invitrogen # 88-8350-88).

Temozolomide cytotoxicity

At 24 hours post-cell seeding, the cells were synchronized by treating with a serum-free medium for 24 hours. After that, cells was treated with 50, 100, 150, and 200 μM temozolomide in a medium containing 10% FBS for 24 hours. Trypan blue exclusion assay was performed to calculate the relative living cell number. Cell viability was analyzed by Microsoft Excel 2013.

Cell proliferation rate

At 24 hours post-cell seeding, GBM cells were collected for counting (0 hour), and other plates were treated with DMSO as the vehicle, 1 μM Paxilline, or 10 μM Cilostazol for 24, 48, or 72 hours. Trypan blue exclusion assay was then performed to calculate the exact cell number.

Electrophysiological measurements

After trypsinization, cells were bathed in normal Tyrode's solution and transferred to a recording chamber mounted on the stage of a CKX-41 microscope (Olympus). The patch electrodes were made of Kimax-51 glass capillaries (Kimble) with a PP-830 electrode puller (Narishige) or a P-97 Flaming/Brown micropipette puller (Sutter), the tips of which were fire-polished with an MF-83 microforge (Narishige). The pipettes had a resistance of 3-5 MW. Patch-clamp recordings were made with the standard patch-clamp technique using an RK-400 amplifier (Biologic). The offset potential between the pipette and the bath solution was compensated with the amplifier.

Data recordings

The signals for both voltage and current tracings were stored on line in a TravelMate-6253 laptop computer (Acer) at 10 kHz through a Digidata-1322A (Molecular Devices). The latter device was equipped with an Adapter SlimSCSI card (Milpitas) and controlled by a pCLAMP 9.2 (Molecular Devices). Current signals were low-pass filtered at 1 or 3 kHZ. pCLAMP-created profiles for rectangular or ramp pulses were frequently used to evaluate current-voltage (I-V) relationships for ion currents. The data were exported to either Origin 8.0 (OriginLab) or a spreadsheet embedded in Microsoft Excel.

Data analysis

Single-channel currents of the BK or IK channels were analyzed by pClamp 9.2 (Molecular Devices). Single-channel amplitudes were determined by fitting Gaussian distributions to the histogram amplitudes of the closed state and open state. The channel activity was defined as $N \times P_0$, which is estimated by the following equation:

$$N \cdot P_0 = \frac{A_1 + 2A_2 + 3A_3 + \cdots + nA_n}{A_0 + A_1 + A_2 + A_3 + A_4 + \cdots + A_n}$$

where N is the number of active channels in the patch, A_0 is the area under the curve of an all-points histogram corresponding to the closed state, and A_1, ..., A_n represent the histogram areas indicating the levels of distinct open state for channel 1 to channel n in the patch examined. The single-channel conductance of either the BK or IK channels was calculated by linear regression using the mean values of the current amplitudes measured at different levels of the holding potentials. Averaged results are presented as means with standard error of the mean (SEM). The Student's t-test and Duncan's multiple-range test for multiple comparisons were performed to articulate the statistical difference among the two or four treatment groups.

Wound healing assay

GBM cells were seeded in 2-chamber culture inserts (ibidi). After the cells reached 90% confluence, the inserts and cultured medium were removed to create a wound. Cells were subjected to different treatments, including 1 μM Paxilline, 10 μM Cilostazol, 1 mM EDTA, and 1 mM KCl (Sigma). The wound area was observed from 0 to 24 hours. Images of the wounds were taken at hour 0 and at different timepoints, the wound areas of which were measured using ImageJ. The migration rate was calculated by the equation: percentage of wound closure = [(wound area at 24 hours)/(wound area at 0 hour)] × 100%.

Transwell assay

GBM cells were seeded in the upper chambers of the Transwell inserts (CORNING), and DMEM with 10% FBS was added into the lower well. After the cells formed a monolayer, serum-free medium with DMSO as the vehicle, 1 μM Paxilline, or 10 μM Cilostazol, was added into the upper chambers to replace the culture medium, and the DMEM with 10% FBS in the lower well was refreshed. The cells were subjected to treatment for nine hours, after which the medium in the upper chamber was discarded and the Transwell inserts were removed from the well. The cells in the upper surface of the Transwell inserts were then removed. The filter was fixed in 4% paraformaldehyde, and the nuclei were stained with hematoxylin (Sigma). The numbers of migratory cells for each filter were then counted.

Tumor sphere formation assay

A low count of cells was suspended in serum-free medium with 1% methyl cellulose, 10 ng/ml EGF, 10 ng/ml bFGF, and B27 supplement. Cells were seeded into 400 µl, non-coating 24-well plates (NEST). Treatments were repeated ten times (1 µM Paxilline or 10 µM Cilostazol) with 10 ng/ml EGF, 10 ng/ml bFGF, and B27 supplement in 40 µl added twice weekly. The cells were treated with Paxilline or Cilostazol for 21 days. The spheres were observed by using an Olympus microscope, the diameters of which were measured by ImageJ software.

Animals

The NOD.CB17-Prkdcscid/NcrCrl (NOD/SCID) mice were purchased from the Laboratory Animal Center, College of Medicine, National Cheng Kung University (NCKU). Five mice were housed in a cage with controlled temperature (22±2°C), humidity (55±5%), and a 12 hours light/dark cycle. The mice were given free access to water and food. Care and use of laboratory animals were in accordance with the National Institutes of Health (NIH) guidelines, and all experimental procedures were approved by the Institutional Animal Care and Use Committee of the College of Medicine, NCKU, with project approval number (#107106 and #109022).

In vivo intracranial xenograft animal model and bioluminescence imaging

1306MG 3.5GR6 and U87MG 2GR4 radiation-resistant human GBM cell lines were transduced with lentiviral vector expressing green fluorescent protein (GFP) and firefly luciferase (Luc). In order to stably express GFP/Luc, antibiotics selection was conducted seven times, after which single cell clones were collected and amplified for further study. The expression of GFP/Luc was checked by immunofluorescent staining for GFP and IVIS for the bioluminescence of luciferase. For tumorigenesis *in vivo*, 5×10^5 Luc-expressing cells in 2 µl were inoculated intracranially into the 8 to 10-week-old male NOD/SCID mice. Mice were anesthetized and placed on a stereotaxic device. A Hamilton syringe with a 30-gauge needle was mounted on a stereotaxic device, and Luc-expressing GBM cells were injected into the right brain (anterioposterior = 0.5 mm, mediolateral = 2.0 mm, and dorsoventral = 3.0 mm from the Bregma). Cilostazol (Cayman) was injected intraperitoneally at a dose of 10 mg/kg twice weekly [18, 19]. Vehicle and Cilostazol treatment started from post-transplantation day 7 to day 52. Tumor growth was monitored by IVIS spectrum Live Imaging System (IVIS-200, Xenogen) twice weekly. Before monitoring, mice were injected with 150 mg/kg D-luciferin (PerkinElmer) and anesthetized with isoflurane. The results of luciferase radiance were quantitated by Live Imaging Software (Xenogen) and the results analyzed using GraphPad Prism software.

Hematoxylin and eosin staining

At the endpoint, whole mice brains were fixed with paraformaldehyde for 3 days at 4°C and processed by standard procedure for paraffin embedding. The paraffin embedded tissues were de-paraffinized by Xylene, followed by rehydration with sequentially reduced ethanol and water. Nuclei and tissue slides were stained by hematoxylin and eosin, respectively. After H&E staining, the slides were dehydrated by ethanol and Xylene, and sealed by mounting medium. These slides were examined using an Olympus Microscope.

Statistics

Each experiment was repeated at least three times. All results are presented as means ± standard error of the mean (SEM). Independent experiments were analyzed by unpaired two-tailed Student's t-test; two-way ANOVA was used to analyze the differences in intracranial tumor growth *in vivo* at different times of treatment. A *p*-value less than 0.05 was considered significant. Microsoft Excel 2013 and GraphPad Prism software were used for statistical calculation and analyses.

Results

Developing radiation resistance in glioblastoma and the potential mechanisms contributing to radiation resistance

Glioblastoma (GBM) cells were irradiated with a dose ranging from 2 to 10 Gy. The median effective dose of radiation (dose of 50% cell viability, ED_{50}) for 1306MG and U87MG were 3.5 Gy and 2 Gy, respectively. On the other hand, the post-irradiated viability was positive-

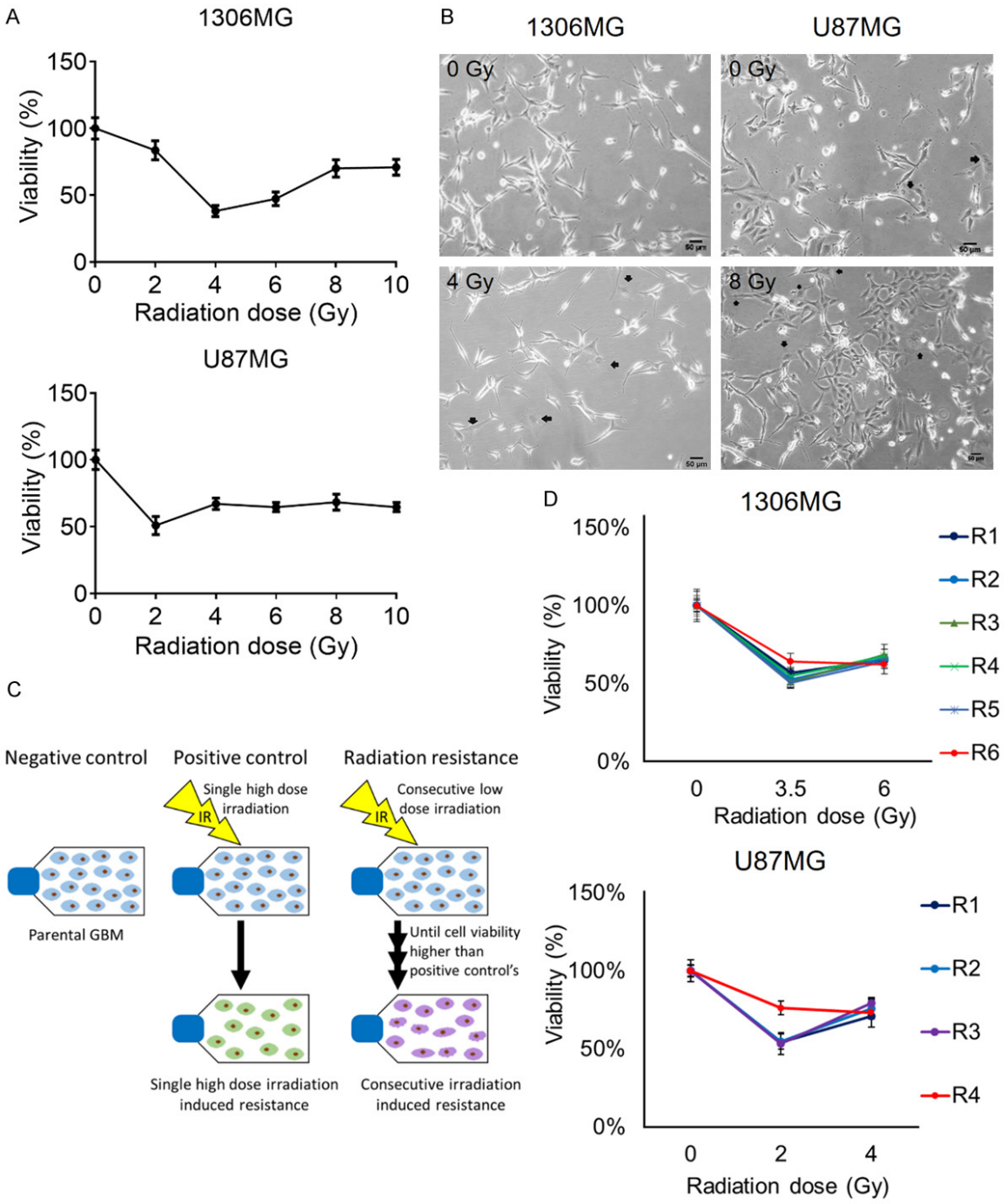

Figure 1. Developing radiation-resistant glioblastoma. A. Cell viability of the post-irradiated 1306MG and U87MG was evaluated by trypan blue exclusion assay; B. The graphs representing the morphology of the 1306MG and U87MG cells. The arrows indicating the altered morphology of the post-irradiated 1306MG and U87MG; C. A schematic presentation indicating a cell model of the developing consecutive irradiation induced resistance in GBM; D. Cell viabilities of the single high-dose irradiated and consecutive irradiated 1306MG and U87MG were evaluated by trypan blue exclusion assay; means ± standard error of the mean (SEM).

ly correlated with increasing dosage, while the irradiation dose was higher than 4 Gy in 1306MG or 2 Gy in U87MG (**Figure 1A**). Irradiation also altered cell morphology, such as irregular shape, enlarged size, multi-nuclei, and loss of processes (**Figure 1B**). Based on the

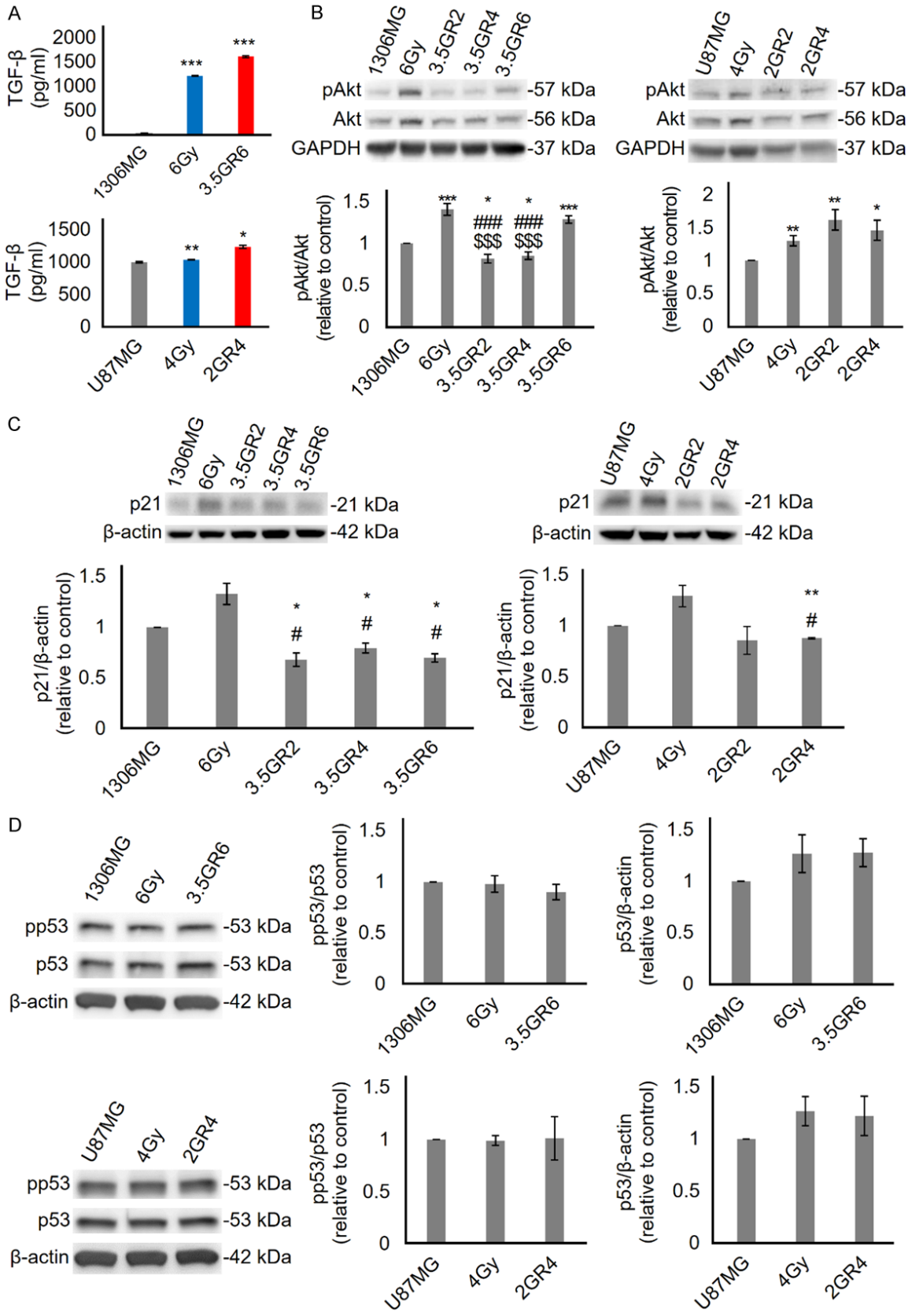

Figure 2. The potential mechanisms confer radiation resistance in GBM. A. The concentration of the total TGF-β in condition medium was measured by enzyme-linked immunosorbent assay (ELISA). Radiation resistance promoted

TGF-β secretion; B. Western blotting (WB) and the histogram showing the ratio of phosphorylated Akt to Akt; C. WB and the histogram showing p21 protein expression; D. WB and the histogram showing the expression of total and phosphorylated p53; means ± SEM; * means comparison with parental GBM; # means comparison with a single high-dose irradiated GBM; $ means comparison with consecutive irradiation induced-resistant GBM; *, P<0.05; **, P<0.01; ***, ###, and $$$, P<0.001.

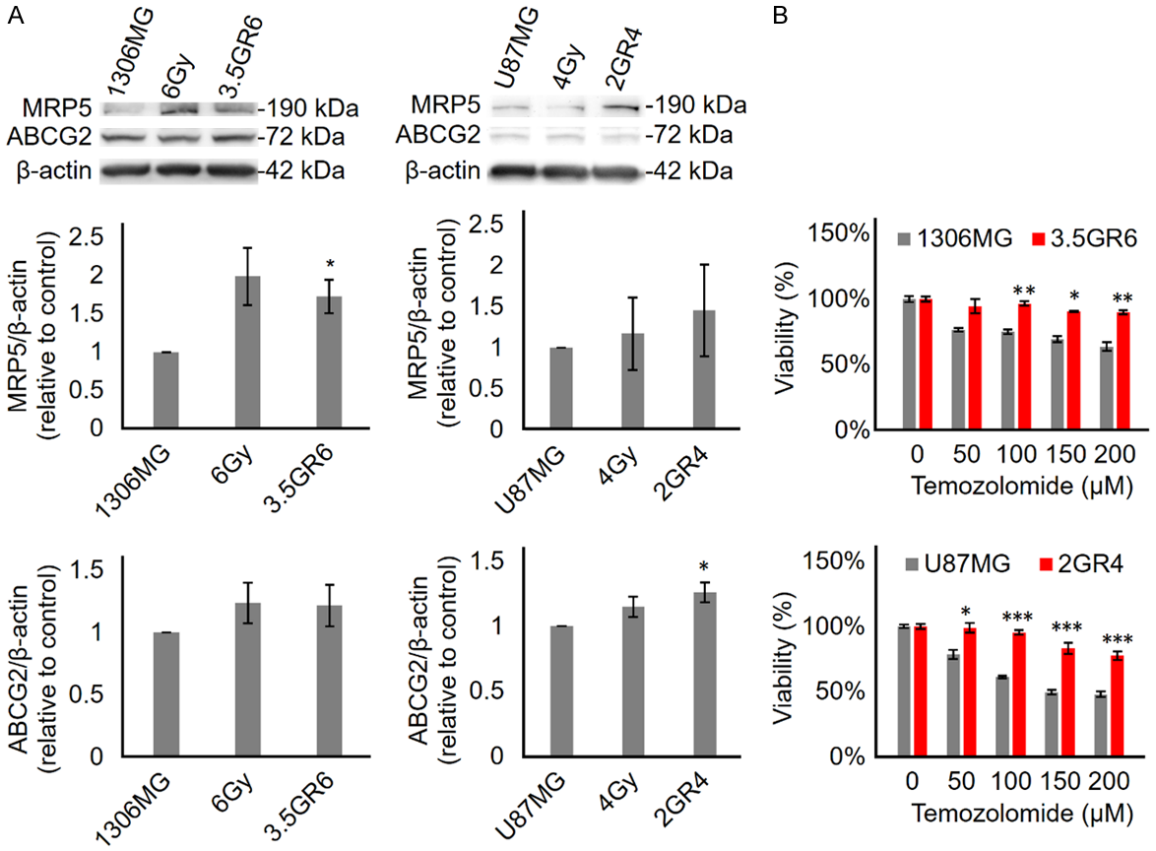

Figure 3. Developing radiation resistance induces drug resistance in GBM. A. WB and the histogram showing the expression of MRP-5 and ABCG2. Developing radiation resistance in 1306MG and U87MG upregulated MRP5 and ABCG2, respectively; B. Cytotoxicity of temozolomide (TMZ) to 1306MG and U87MG was evaluated by trypan blue exclusion. Radiation resistance enhanced resistance against TMZ; means ± SEM; * means comparison with parental GBM; *, P<0.05; **, P<0.01; ***, P<0.001.

post-irradiated viability and modified method from Yan et al., ED_{50} was selected for developing the consecutive irradiation-induced resistance (CIIR) [16]. The cells subjected to a single high-dose of irradiation (6 Gy for 1306MG and 4 Gy for U87MG) were selected to evaluate "when" CIIR was established. When the viability of the consecutive-irradiation group was higher than that of the single high-dose irradiation group, it was defined as radiation-resistant GBM (**Figure 1C**). Accordingly, in order to develop CIIR, six exposures to 3.5 Gy irradiation were required for 1306MG (referred to as 3.5GR6), and four exposures of 2 Gy irradiation were required for U87MG (referred to as 2GR4) (**Figure 1D**).

Various mechanisms are involved in radiation resistance, including evoking anti-death/pro-survival pathways, DNA damage repair, senescence, inflammatory cytokines, and epithelial-mesenchymal transition (EMT) [20]. Transforming growth factor-β (TGF-β) contributes to cancer progression via regulating apoptosis, modulating the immune system, inducing EMT, and promoting metastasis [21-23]. Also, cancer cells develop resistance against radiotherapy by increasing and activating TGF-β signaling [24-26]. Akt is one of the key pro-survival mediators in radiation response. Tumors survive the radiation damage and cell death via activating Akt signaling [4, 27]. In our approach, CIIR and single high-dose irradiation enhanced TGF-β

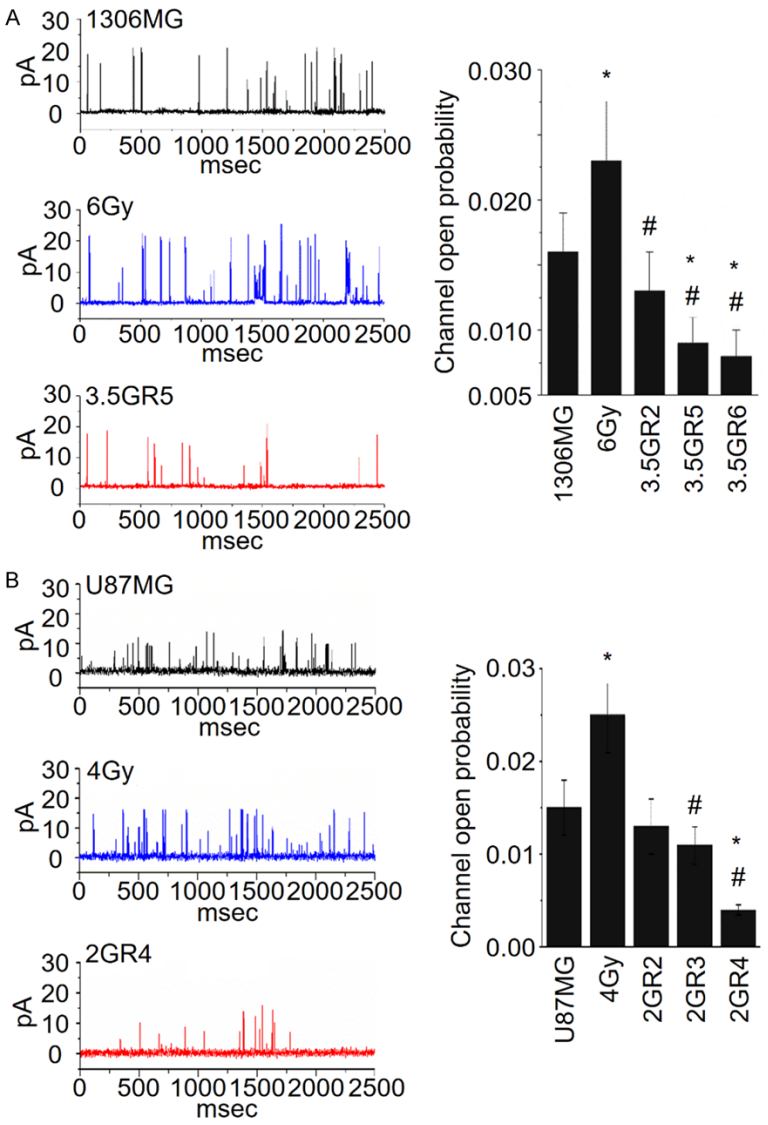

Figure 4. Developing consecutive irradiation-induced resistance reduces BK channel activity. A. The currents and open probability of BK channels in parental, single high-dose irradiated, and consecutive irradiated 1306MG. Developing radiation resistance in 1306MG significantly reduced BK channel activity; B. The currents and open probability of BK channels in parental, single high-dose irradiated, and consecutive irradiated U87MG. Developing radiation resistance in U87MG decreased BK channel activity; * means comparison with parental GBM; # means comparison with single high-dose irradiated GBM; means ± SEM; * and #, P<0.05.

secretion (**Figure 2A**) and Akt activation (**Figure 2B**). p21 is a well-establish factor that participates in regulating cell growth, genomic stability, and senescence. p21 also exerts functions in a p53-dependent or independent manner [28]. In our model, CIIR downregulated p21 expression (**Figure 2C**) without changing the expression of total and phosphorylated p53 (**Figure 2D**). Thus, the roles of p21 in radiation resistance is p53-independent. Additionally, in a combined therapy procedure, chemotherapy produced a good response initially; however, when cancers develop radiation resistance, they also gain drug resistance by enhancing the expression of multidrug-resistant proteins [29]. Specifically, we found that CIIR significantly increased the multidrug-resistant proteins MRP5 and ABCG2 in 1306MG and U87MG, respectively (**Figure 3A**). Moreover, compared with parental GBM, the CIIR GBM become resistant to temozolomide (**Figure 3B**). These observations confirmed that our model could be utilized to further investigate radiation resistance.

Consecutive irradiation-induced resistance diminishes BK channel activity in an expression-independent manner

Due to a strong correlation between calcium-activated potassium channels and cancer progression, we first detected and recorded calcium-activated potassium channels by patch clamp with single-channel and whole-cell recording simultaneously. A single high-dose of irradiation enhanced BK channel activity; by contrast, in consecutive irradiation groups, irradiation did not alter BK channel activity initially (1306MG 3.5GR2 and U87MG 2GR3). However, BK channel activity was significantly reduced when GBM developed CIIR (**Figure 4A**, **4B**). On the other hand, the dose and frequency of irradiation did not affect the activity of the IK channels (**Figure 5**); meanwhile, SK channel activity was not detected.

A BK channel consists of α channel subunits (BK channel) and β regulatory subunits (BKβ), the latter of which regulate BK-channel activity

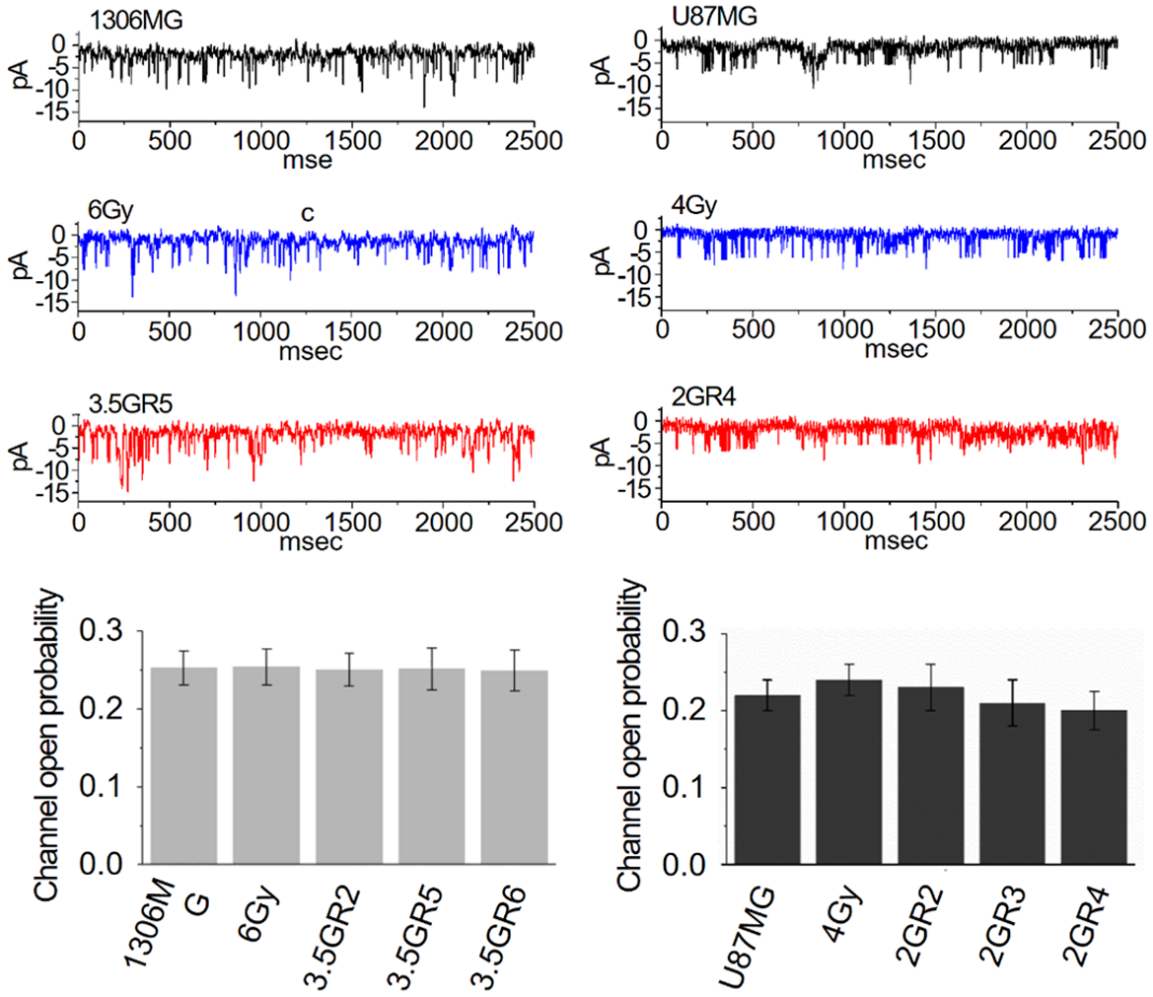

Figure 5. Consecutive irradiation-induced resistance does not affect the activity of the IK channel. The currents and open probability of the IK channels in parental, single high-dose irradiated, and consecutive irradiated GBM cells; means ± SEM.

by modulating calcium sensitivity or via cytosolic signaling [30]. In single high-dose irradiation, BK channel expression was significantly upregulated. Intriguingly, the expression of BK channels was increased before GBM developed CIIR (1306MG 3.5GR1 to 3.5GR5 and U87MG 2GR1 to 2GR3). When GBM developed CIIR, the BK channel expression remained unchanged or slightly decreased (**Figure 6A**). Only in single high-dose irradiated 1306MG did BKβ increase, whereas CIIR did not alter BKβ expression (**Figure 6B**).

Paxilline is a BK channel-specific inhibitor that does not affect the IK and SK channels. Cilostazol, a type III phosphodiesterase inhibitor, is able to activate the BK channel. Accordingly, we used Cilostazol and Paxilline to activate and inhibit BK channel activity, respectively. In **Figure 7**, Cilostazol was able to re-activate BK channels, while Paxilline inhibited Cilostazol-induced BK channel activity.

Cilostazol inhibits radiation resistance-induced cell migration

Radiation resistance promotes tumor malignancy, including enhancing migration, invasion, and proliferation. Wound healing assay is a convenient approach to evaluating two-dimensional (2D) migration. Compared with parental GBM cells, CIIR promoted cell migration in 1306MG (71.3±3.5% vs. 53.3±4.3%, P = 0.0012) and U87MG (85.7±1.5% vs. 81.8± 1.5%, P = 0.0480). In the parental GBM cells, the blockade of BK channels induced by Paxilli-

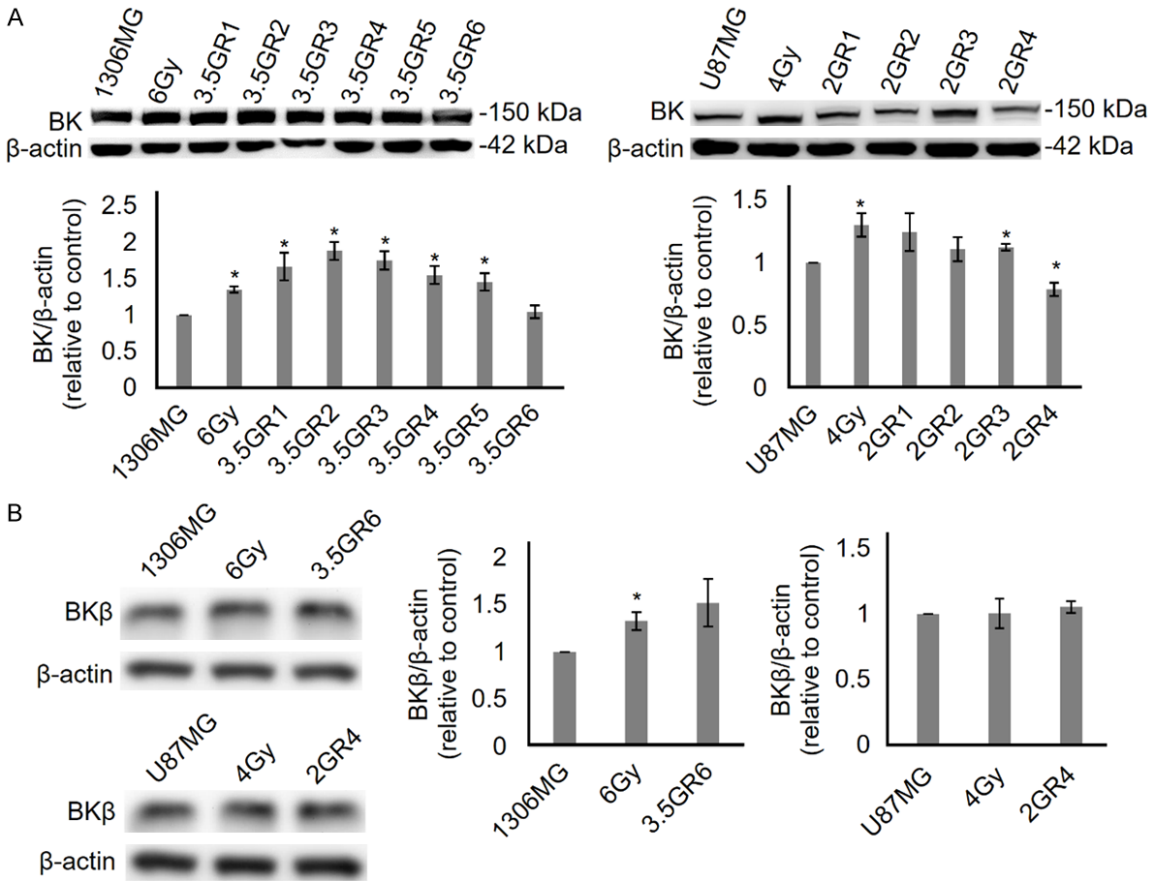

Figure 6. Developing radiation resistance does not alter protein expression of the BK channel and its cytoplasmic regulatory subunit BKβ. A. WB and the histogram showing the protein expression of the BK channel; B. WB and the histogram showing the protein expression of the regulatory β subunit of the BK channel (BKβ); means ± SEM; * means comparison with parental GBM; *, P<0.05.

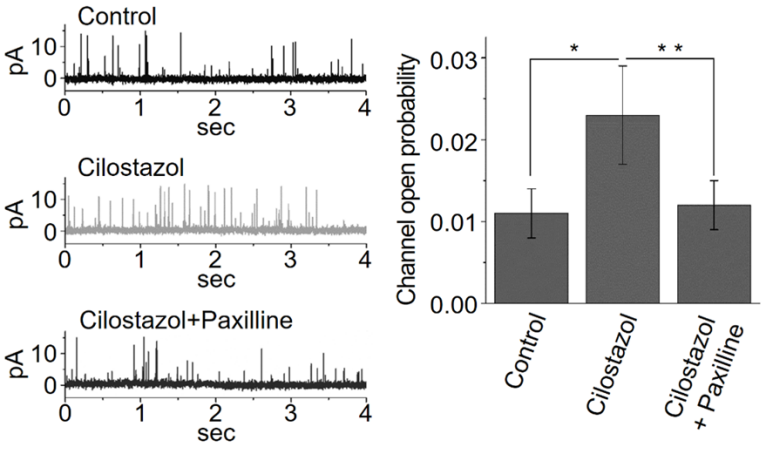

Figure 7. Cilostazol re-evokes consecutive irradiation resistance-diminished BK channel activity. The currents and open probability of the BK channels of 1306MG irradiated five times with 3.5 Gy (3.5GR5). Cilostazol directly activated BK channels while Paxilline specifically blocked the BK channels; * means comparison with Cilostazol treatment; means ± SEM; *, P<0.05; **, P<0.01.

ne accelerated 2D migration (71.3±3.5% vs. 63.7±2.9%, P = 0.0451 for 1306MG; 85.7±1.5% vs. 79.8±2.3%, P = 0.04995 for U87MG), while Cilostazol did not affect cell migration (73.1±3.5%, P = 0.6309 for 1306MG; 85.7± 1.4%, P = 0.9692 for U87-MG). In contrast, Cilostazol significantly slowed CIIR-induced cell migration in 1306-MG and U87MG (53.3±4.3% vs. 62.5±3.3%, P = 0.0474 for 1306MG 3.5GR6; 81.8± 1.5% vs. 86.0±1.2%, P = 0.0250 for U87MG 2GR4), while Paxilline did not affect the cell migration of the CIIR GBM cells (52.2±1.8%, P =

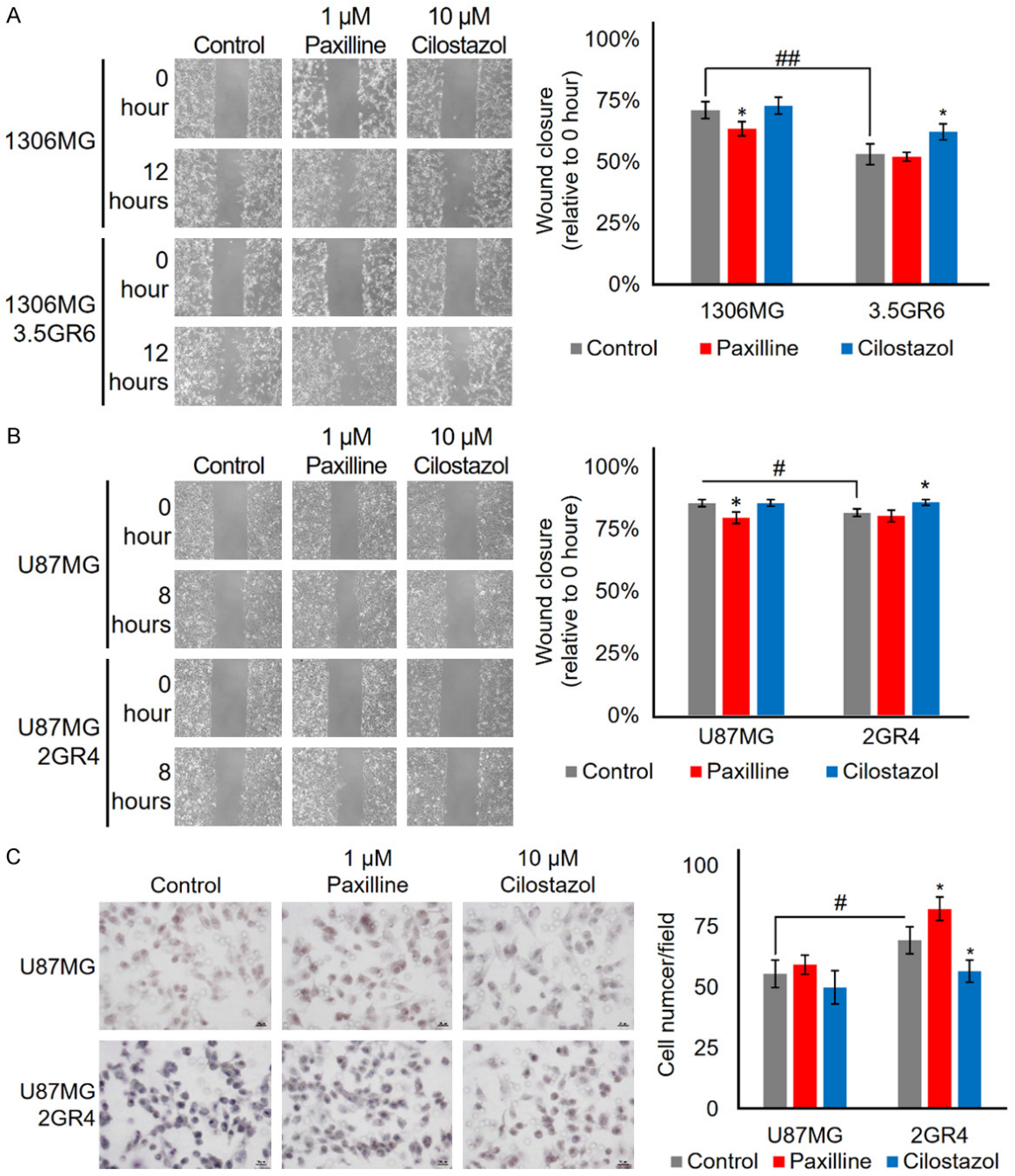

Figure 8. Re-evoking the BK channels inhibits the migration ability of radiation-resistant GBM. A. **Paxilline and Cilostazol** were used to inhibit and activate the BK channels, respectively. Two-dimension (2D) migration ability was evaluated by wound-healing assay. The histogram showing the proportion of wound closure of 1306MG. N = 4; B. The graphs and the histogram showing the ability of 2D migration of U87MG. N = 4; C. Three-dimension migration ability was evaluated by transwell assay. The histogram indicating the number of migratory cells in differential BK channel activity. N = 5; means ± SEM; * means comparison with control; # means comparison with the control of parental GBM; * and #, P<0.05.

0.7670 for 1306MG 3.5GR6; 80.5±2.3%, P = 0.5452 for U87MG 2GR4) (**Figure 8A**, **8B**).

Three-dimensional (3D) migration was evaluated by transwell assay. The results of 3D migration were similar to those of 2D migration, namely CIIR increased the 3D migratory ability (55.7±5.6 vs. 69.5±5.6, P = 0.0489). Although Paxilline only slightly increased the cell mobility of the parental U87MG cells (55.7±5.6 vs.

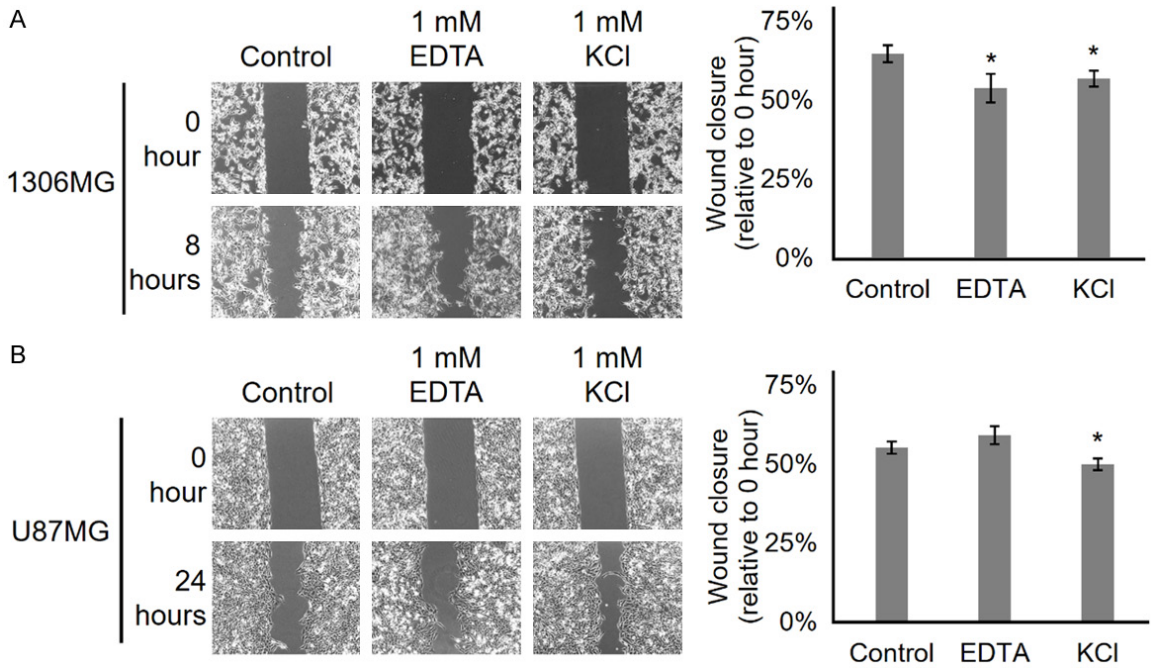

Figure 9. Inhibiting BK channels by modulating the extracellular potassium and calcium concentration affects GBM migration. A. Potassium Chloride (KCl) and Ethylenediaminetetraacetic acid (EDTA) were used to increase and chelate calcium, respectively. The 2D migration ability was evaluated by wound-healing assay. The histogram showing the proportion of wound closure for the 1306MG. N = 3; B. The graphs and histogram showing the ability of 2D migration for the U87MG. N = 4; means ± SEM; * means comparison with control; *, P<0.05.

59.5±3.9, P = 0.2922), it significantly enhanced the cell mobility of radiation-resistant U87-MG 2GR4 (69.5±5.6 vs. 82.4±4.8, p = 0.0494). Meanwhile, Cilostazol inhibited only CIIR-induced cell migration (69.5±5.6 vs. 56.8±4.6, P = 0.0480) (**Figure 8C**).

BK channels can be activated by calcium flux and allow for potassium to flow outward. Therefore, in order to elucidate the role of potassium currents via BK channels in cell migration, potassium chloride (KCl) and Ethylenediaminetetraacetic acid (EDTA) were utilized to increase extracellular potassium and chelate calcium, respectively, to inhibit outward potassium currents. In our 2D migration model, chelating calcium by EDTA promoted only cell migration of the parental 1306MG (64.8±2.6% vs. 53.8±4.5%, P = 0.0334) (**Figure 9A**); EDTA did not affect the 2D migration of the parental U87MG (55.4±2.0% vs. 59.3±2.8%, P = 0.2227) (**Figure 9B**). Increasing extracellular potassium by KCl to block the outward potassium current promoted the cell motility of parental 1306MG and U87MG (64.8±2.6% vs. 56.9±2.6% for 1306MG; 55.4±2.0% vs. 50.0±1.8% for U87-MG) (**Figure 9A**, **9B**). These findings indicate that BK channel inactivation confers radiation resistance in GBM via promoting cell mobility. On the other hand, Cilostazol suppresses CIIR-induced cell migration by re-evoking BK channels.

Cilostazol reduces cell proliferation and inhibits tumor sphere formation

Acquisition of resistance not only allows GBM to survive treatment, but also leads to uncontrolled tumor growth and induces cancer stem-cell properties. Compared with parental cells, GBM cells with CIIR significantly accelerated the cell-proliferation rate. In parental 1306MG cells, although the Paxilline-induced blockade of BK channels increased cell proliferation, Paxilline did not change the cell proliferation of the parental U87MG cells. In addition, Cilostazol did not affect the cell proliferation of parental GBM cells. In the CIIR 1306MG and U87MG, Paxilline did not affect cell proliferation; however, Cilostazol significantly inhibited radiation resistance-induced cell proliferation (**Figure 10A**, **10B**). Furthermore, Cilostazol attenuated the ability to form CIIR tumor spheres by reducing their diameter (122.8±6.8 μm vs. 82.1±3.9

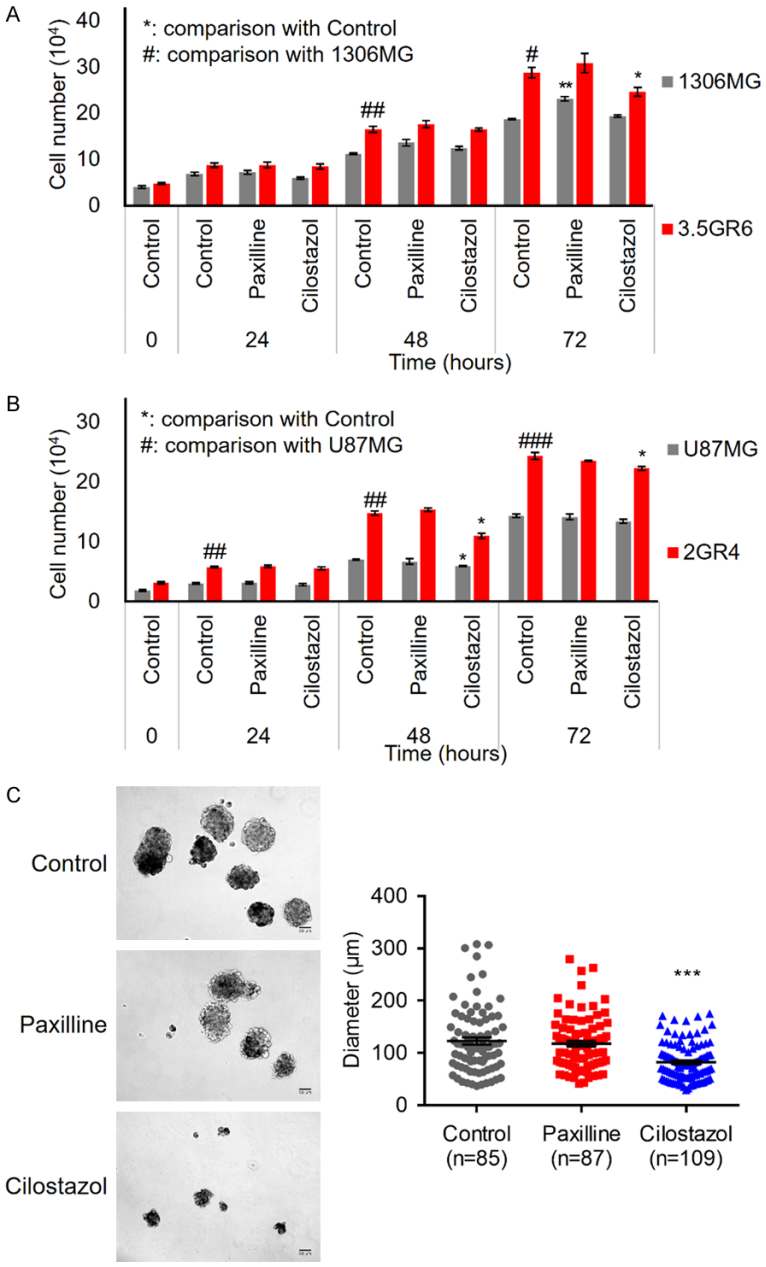

Figure 10. Effects of modulating BK channel activity on cell growth. A, B. Paxilline and Cilostazol were used to inhibit and activate BK channels, respectively. The histogram showing the alternation of the cell proliferation rate of 1306MG and U87MG; means ± SEM; * means comparison with control; # means comparison with parental GBM; * and #, P<0.05; ** and ##, P<0.01; *** and ###, P<0.001; C. The graphs indicating tumor-sphere formation of radiation-resistant 1306MG 3.5GR6 cells. The histogram showing the diameter of the tumor spheres. Cilostazol significantly inhibited the capacity of tumor-sphere formation. * means comparison with control; ***, P<0.001.

μm, P<0.0001), while Paxilline had no effect on the diameter of the CIIR tumor spheres (122.8±6.8 μm vs. 117.8±5.4 μm, P = 0.7267) (**Figure 10C**).

Accordingly, the decrement of BK channel activity in GBM not only contributes to the facilitation of radiation-resistant cell migration, it also leads to accelerated cell proliferation and induced cancer stemness.

Cilostazol suppresses radiation-resistant GBM growth in an intracranial model

We further clarified the antitumor effects of Cilostazol on radiation-resistant GBM under *in vivo* conditions by using an intracranial injection model. Luciferase-expressing radiation-resistant U87-MG 2GR4 cells (5 × 10^5 cells in 2 μl) were injected intracranially into NOD/SCID mice. The tumor growth was monitored by an IVIS-200 bioluminescence image system. At day 7 post-transplantation, Cilostazol (10 mg/kg) or Dimethyl sulfoxide (DMSO) as a vehicle was injected intraperitoneally twice per week into the mice and tumor growth was observed for 47 days. Compared with the vehicle groups, **Figure 11A** shows that Cilostazol delayed radiation-resistant U87MG 2GR4 growth. A two-way ANOVA revealed a main effect of Cilostazol vs. vehicle ($F(1,103) = 19.36$, $P<0.0001$), interaction ($F(13,103) = 2.738$, $P = 0.0023$) and days after treatment ($F(13,103) = 7.131$, $P<0.0001$) (**Figure 11B**). A Kaplan-Meier analysis of the survival of the vehicle- and Cilostazol-treated mice is displayed in **Figure 11C**. The median survival of the vehicle control was 46.5 days while the median survival of the Cilostazol-treated group was undefined. As shown in **Figure 11D**, compared with the vehicle control, the Cilostazol treatment did

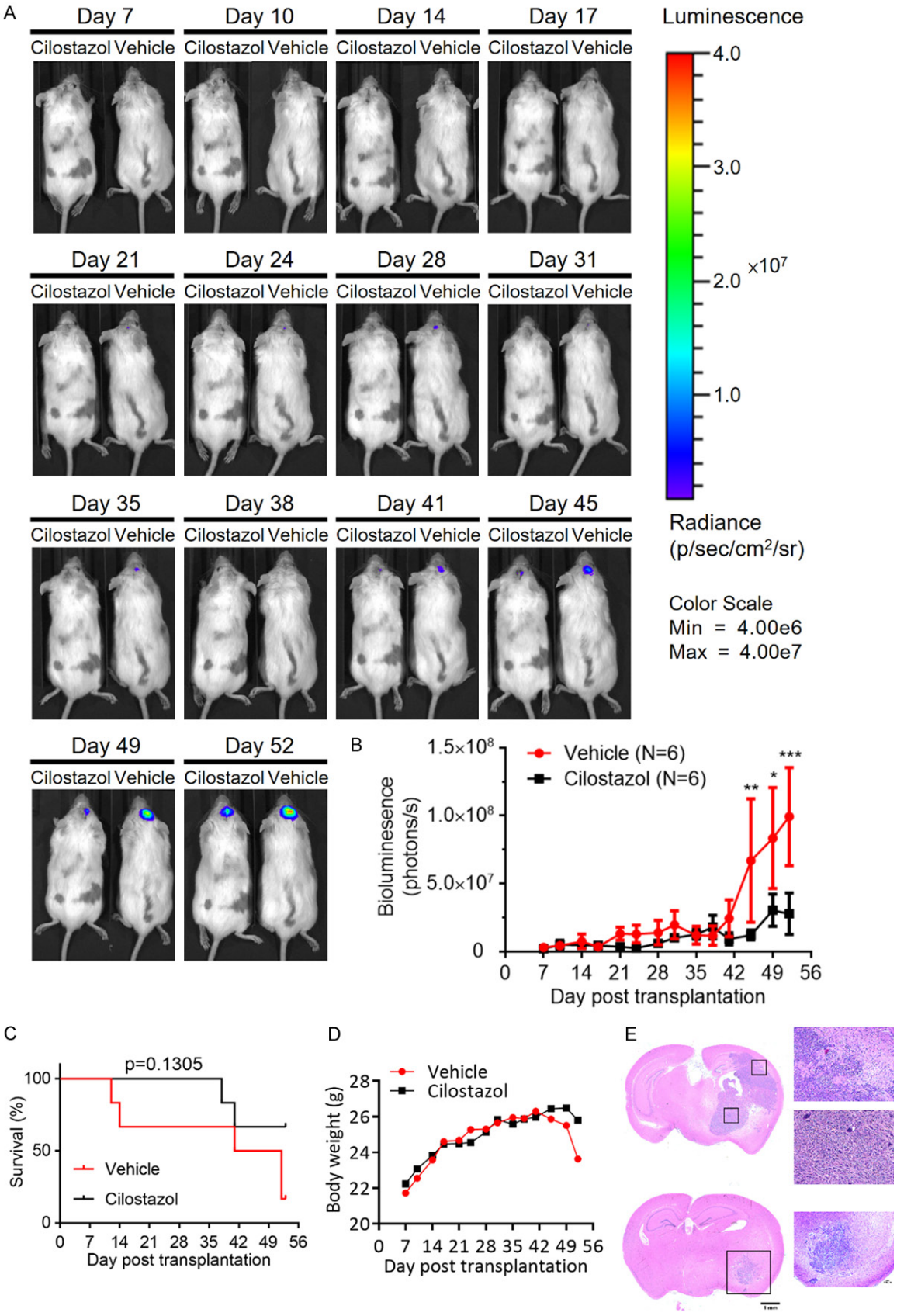
A
Day 7
Day 10
Day 14
Day 17
Day 21
Day 24
Day 28
Day 31
Day 35
Day 38
Day 41
Day 45
Day 49
Day 52
Cilostazol Vehicle
Luminescence
4.0
3.0
2.0
1.0
×10⁷
Radiance
(p/sec/cm²/sr)
Color Scale
Min = 4.00e6
Max = 4.00e7
B
Vehicle (N=6)
Cilostazol (N=6)
Bioluminescence (photons/s)
1.5×10⁸
1.0×10⁸
5.0×10⁷
0
**
*
***
0 7 14 21 28 35 42 49 56
Day post transplantation
C
p=0.1305
Survival (%)
100
50
0
Vehicle
Cilostazol
0 7 14 21 28 35 42 49 56
Day post transplantation
D
Vehicle
Cilostazol
Body weight (g)
28
26
24
22
20
0 7 14 21 28 35 42 49 56
Day post transplantation
E

Figure 11. Cilostazol delays radiation-resistant U87MG 2GR4 growth and prolongs survival in an intracranial tumor model. A. Luciferase (Luc)-expressing radiation-resistant U87MG 2GR4 cells (5×10^5 cells) were injected intracranially into the striatum of the NOD-SCID mice. Tumor growth was monitored by using the IVIS-200 imaging system; B. The histogram indicating tumor growth by evaluating bioluminescent photons. Tumor growth was slower in the Cilostazol-treated mice than in the vehicle-control mice; means ± SEM; n = 6 in vehicle and Cilostazol groups; * means comparison with vehicle control, *, P<0.05; **, P<0.01; ***, P<0.001; C. Kaplan-Meier survival curve of the vehicle- and Cilostazol-treated mice; D. The histogram indicating the changes of body weight. As seen, Cilostazol did not alter the body weight; E. Hematoxylin and eosin staining showing the morphology of the GBM. Tumors of the vehicle-treated mice were significantly larger than those of the Cilostazol-treated mice.

not affect the body weight of the mice. A two-way ANOVA indicated a main effect of Cilostazol vs. vehicle ($F(1,104) = 0.3055$, $P = 0.5816$), interaction ($F(13,104) = 0.1809$, $P = 0.9993$) and days after treatment ($F(13,104) = 3.083$, $P = 0.0007$). The tumor growth in the brain was analyzed in coronal brain slices by hematoxylin and eosin staining. The slices revealed that the tumor size of the Cilostazol-treated mice was smaller than that of the vehicle-treated mice (**Figure 11E**). In order to confirm that the anti-tumor effects of Cilostazol was not cell-line specific, luciferase-expressing radiation-resistant 1306MG 3.5GR6 cells (5×10^5 cells in 2 μl) were injected intracranially into the NOD/SCID mice. The same procedures of vehicle and Cilostazol treatment and tumor-growth monitoring by IVIS were applied to the 1306MG 3.5GR6 *in vivo* growth. As shown in **Figure 12A** and **12B**, Cilostazol inhibited tumor growth. Also, Cilostazol did not affect the body weight of the 1306MG 3.5GR6 transplanted mice (**Figure 12C**).

Discussion

The underlying mechanisms of developing radiation-resistance

Radiation therapy is the first-line adjuvant therapy following surgical debulking in GBM therapy. Consecutive irradiation with 1.8 to 2.2 Gy radiation and a total dose of up to 60 Gy is therapeutic [31]. However, radiotherapy only shows moderate efficacy. Developing radiation resistance is a complicated process involving activating adaptive pathways, evoking anti-death/pro-survival pathways, DNA damage repair, senescence, inflammatory cytokines, EMT, and inducing the properties of cancer stem cells. Furthermore, radiation resistance might enhance drug resistance. Irradiation leads to cell death primarily via causing DNA double-strand breaks. Under consecutive treatments, tumor cells accumulate gene mutations and accelerate the DNA repair rate, which results in genomic instability and resistance [7]. Conventionally, p21 is regarded as a tumor suppressor by sustaining genomic stability and controlling cell-cycle arrest. p21 exerts as a p53 downstream effector to assist DNA repair. By inhibiting cyclin-dependent kinase, p21 determines cell fate to apoptosis or senescence [32, 33]. In general, in order to proliferate, cancers overcome cell-cycle arrest by attenuating p21 expression [34]. In well-differentiated tissues, p53 is required for stress responses by p21, such as post-irradiated DNA repair or apoptosis [28, 35]. However, accumulated evidence has shown that p21 is able to regulate biological processes in a p53-independent manner. The expression of p21 is higher in differentiated tissues than in embryonic tissues. When cells exert differentiation, the cell cycle slows down and is accompanied by upregulated p21 in a p53-independent manner. For instance, myoblast differentiation occurs with p21 induction [36]. Otherwise, under a p53-absent condition, p21 was reported to respond to starvation/serum release, and tissue differentiation [36]. EMT is an important process in cancer progression. It enhances the abilities of tumor migration, invasion, and cancer stemness. That is, EMT is similar to the process of de-differentiation. TGF-β is a multifunctional cytokine contributing to cancer progression and is a well-known inducer of EMT. Cancer cells developing radioresistance typically feature incremental activation of TGF-β signaling [24-26]. As GBM is irradiated, the accumulating TGF-β confers resistance [21-23, 37]. Also, blocking TGF-β enhances the radiation efficacy for GBM [26, 38]. Accordingly, in a p53-independent situation, by downregulating p21 expression and facilitating TGF-β signaling, the radiation resistance developed in GBM is able to promote EMT, de-differentiate into cancer stem cells, and enhance various malignancies. On the other hand, under irradiation, tumor cells activate Akt signaling to prevent cell death by facilitat-

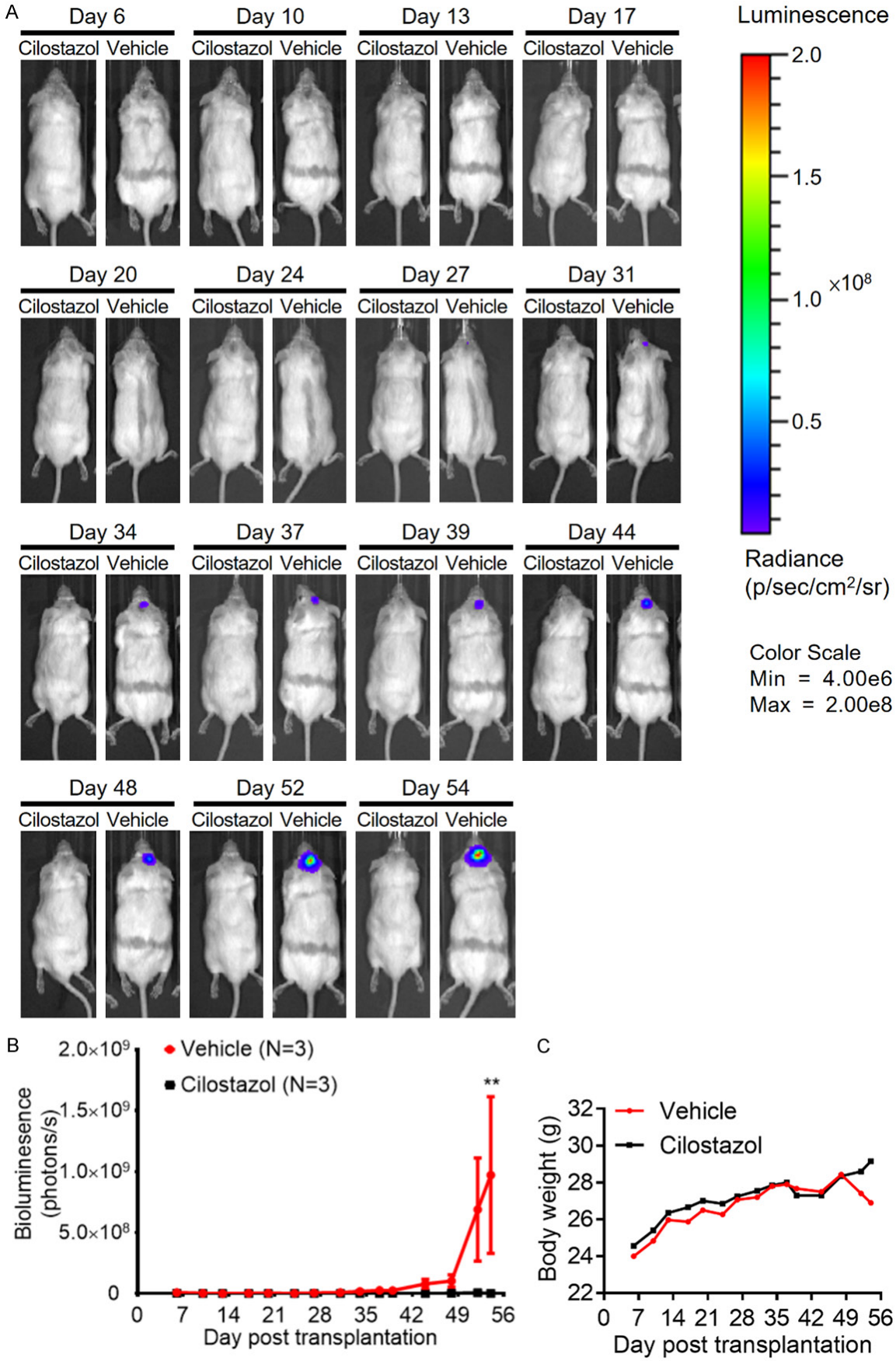
A
Day 6
Day 10
Day 13
Day 17
Day 20
Day 24
Day 27
Day 31
Day 34
Day 37
Day 39
Day 44
Day 48
Day 52
Day 54
Cilostazol
Vehicle
Luminescence
2.0
1.5
1.0
×10^8
0.5
Radiance
(p/sec/cm²/sr)
Color Scale
Min = 4.00e6
Max = 2.00e8
B
Vehicle (N=3)
Cilostazol (N=3)
**
Bioluminesence
(photons/s)
2.0×10^9
1.5×10^9
1.0×10^9
5.0×10^8
0
0 7 14 21 28 35 42 49 56
Day post transplantation
C
Vehicle
Cilostazol
Body weight (g)
32
30
28
26
24
22
0 7 14 21 28 35 42 49 56
Day post transplantation

Figure 12. Cilostazol inhibits radiation-resistant 1306MG 3.5GR6 growth in an intracranial tumor model. A. Luc-expressing radiation-resistant 1306MG 3.5GR6 cells (5×10^5 cells) were injected intracranially into the striatum of NOD-SCID mice. Tumor growth was monitored using an IVIS-200 imaging system; B. The histogram indicating tumor growth by evaluating bioluminescent photons. Tumor growth was slower in the Cilostazol-treated mice than in the vehicle-control mice; means ± SEM; n = 3 in vehicle and Cilostazol groups; * means comparison with vehicle control; **, $P<0.01$; C. The histogram indicating the changes of body weight. Cilostazol did not alter the body weight.

ing cell proliferation and invasion [4, 7, 39]. In contrast, inhibition of Akt promotes the radiation response [40]. Furthermore, after radiation therapy, the efficacy of chemotherapy lessens [29]. Drug resistance can be intrinsic or inducible, but these two pathways share the common feather of highly-expressed or upregulated multidrug-resistant proteins (MRPs). Inducible drug resistance results from long-term drug treatment or other external stimulation, such as traditional radiotherapy and hypoxic condition. Gradually, tumors may enhance the expression of MRPs leading to a loss of sensitivity to anti-tumor agents [41]. In our model, developing radiation resistance by consecutive irradiation of GBM is accompanied by enhanced TGF-β secretion, reduced p21 expression in a p53-independent manner, activated pro-survival Akt signaling, and promoted temozolomide resistance by upregulating MRPs. Also, radiation resistance in GBM increases the post-irradiation viability, enhances cell mobility, and facilitates cell proliferation. Based on this evidence, our model displayed various characteristics of radiation resistance. Accordingly, it is possible to display the authentic status of radiation resistance in GBM.

The role of BK channels in radiation resistance

Calcium-activated potassium channels with big conductance (BK channels) are not only ubiquitously expressed in normal tissues, but highly expressed in various cancers. The main function of BK channels is to control the outward flow of potassium, which modulates cell membrane potential, cell volume, shape, migration, invasion, and proliferation [42]. BK channels can be activated by calcium flux, cytoplasmic signaling, and the alternation of membrane potential. However, the role of BK channels in tumor biology remains controversial. BK channels are highly expressed in breast cancers, where the BK channel opener induces caspase-3 dependent apoptosis in triple-negative breast cancer cells [43]. Ionizing irradiation immediately activates BK channels, which may lead to cell shrinkage; afterward however, cells swell back to normal or a larger size [44]. Irradiation-induced BK channel activation promotes cancer mobility, leading to radiotherapy failure [14, 45]. Additionally, blocking BK channels enhances radiation responses leading to cell death in GBM [46]. However, Kraft et al. demonstrated that enhanced BK channel activity decreases cell mobility. BKβ regulates the channel activity by sensitizing calcium, BK channel trafficking, or their interplay with cytosolic factors [47, 48]. Steinle et al. showed that ionizing radiation activates BK channels, in which the entry of calcium was increased or decreased to affect the cell mobility [14]. BK channel-regulating cell migration may even be calcium-independent [49]. The effects of BK-channel activity on migration are varied; that is, it may increase, decrease, or not change, depending on the types of cells, tissues, and stimuli [50-52]. Stimuli facilitate the activation of BK channels while the expression is instead unchanged [53]. Additionally, the expression of BK channels inversely correlates with drug resistance. Compared with drug-sensitive tumor cells, the expression of BK channels is low in resistant tumors. A knockdown of BK channels or blocking BK channels with Paxiline is able to enhance cisplatin resistance in ovarian cancers [54]. These findings indicated that BK channels may not only contribute to cell migration, but they might also confer therapeutic resistance. However, the role of BK channels in different cancers may be tissue- and cell-specific. As such, further studies are needed, especially in therapeutic-induced resistance.

While cells are stimulated or require to increase proliferation rate, it enhances fermentative metabolism (glycolysis) to generate more ATP and lactate. This metabolic shift from mitochondrial oxidative phosphorylation to cytosolic aerobic glycolysis is known as Warburg effect [55, 56]. Otherwise, the microenvironment of tumors presents hypoxic. Hypoxia is able to promote glycolysis which produce more lactate to acidify the microenvironment [57]. In return, glycolysis stabilizes hypoxia responding protein HIF1α. It appears positive feedback to promote

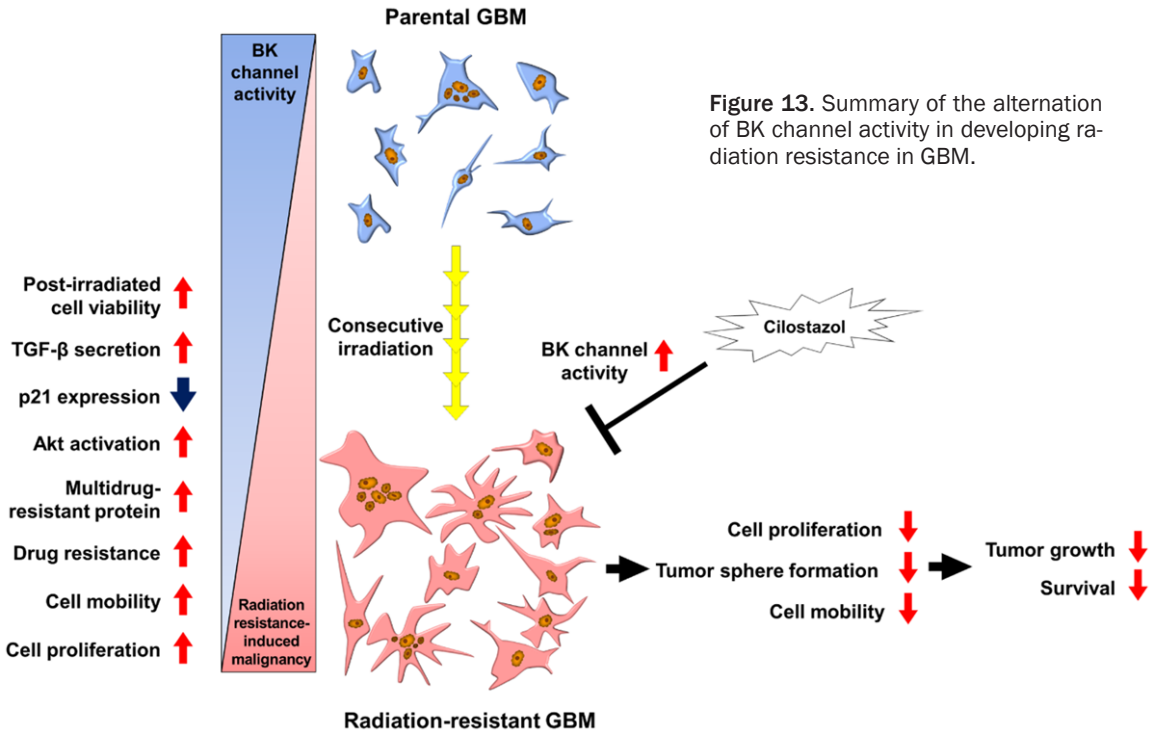

Figure 13. Summary of the alternation of BK channel activity in developing radiation resistance in GBM.

tumor progression. In addition, BK channels can be inhibited by extracellular acidification [58]. In our findings, consecutive irradiation-induced resistance accelerated cell proliferate rate. The requirement of ATP for faster proliferation may prefer Warburg effect instead of oxidative phosphorylation which leads to extracellular acidification. Consequently, the activity BK channels was blocked in protein expression-independent and cytoplasmic regulation-independent manners.

The anti-tumor effects of cilostazol

Cilostazol, a selective cyclic AMP (cAMP) phosphodiesterase inhibitor, is a common drug for treating vascular diseases, such as stroke and peripheral vascular disease. The anti-platelet and anti-thrombotic effects of Cilostazol result from inhibiting cAMP degradation. Protein kinase A (PKA) is a well-known intracellular cAMP receptor. Elevating cAMP activates PKA to regulate various biological processes, including cell metabolism, gene expression, and intracellular calcium; however, cAMP suppression leads to brain tumor initiation and progression. Xinget al. reported that elevating cAMP production by activating adenyl cyclase or inhibiting phosphodiesterases forces GBM cell differentiation into normal-like glia cells and attenuates cancer stemness. Furthermore, increasing cAMP effectively inhibits GBM *in vivo* growth [59]. On the other hand, depending on the cell type, Cilostazol can open BK channels by directly activating them or regulating cytoplasmic cAMP/PKA signaling, with Cilostazol-induced vasodilation able to occur via endothelial and smooth muscle cells. Cilostazol activates BK channels through the production of nitric oxide in endothelial cells, while in smooth muscle cells, it opens BK channels via cAMP/PKA signaling [60]. In addition, electrophysiological observation revealed that Cilostazol was able to activate BK channels immediately without increasing intracellular calcium and cytosolic substance. That is, the stimulatory effects of Cilostazol might directly bind to the intracellular gating site of the BK channels [17, 61]. Based on previous studies and our findings, Cilostazol holds high potential to function as a coadjuvant therapy with conventional radio-, chemo-, or radiochemotherapy. Mechanically, Cilostazol is able to eradicate radiation-resistant GBM via directly activating BK channels or via cAMP signaling.

Conclusion

Radiation is a common therapy for cancers, especially for GBM. However, despite the good initial response, cancers eventually overcome radiation damage and develop resistance. In

summary, we established a reliable experimental model to monitor the development of radiation resistance in GBM. In addition, our findings revealed that developing radiation resistance diminishes BK-channel activity in a protein expression-independent manner. Re-evoking BK channel activity by Cilostazol can inhibit radiation resistance-induced cell migration, proliferation, tumor-sphere formation, and *in vivo* growth (**Figure 13**). That is, Cilostazol has the potential to improve the therapeutic efficacy for GBM. Furthermore, combining conventional radiation therapy or radiochemotherapy with Cilostazol or other BK channel activators (such as anti-asthmatic agent Adolast, BMS-191011, NS19504, and NS11021) may overcome therapeutic resistance and be an effective strategy for GBM therapy.

Acknowledgements

The authors would like to thank Yan-Ming Huang for the technical support of electrophysiological measurements, Hsiao-Wen Chiu for irradiating the GBM cell lines, Dr. Yang-Kao Wang for providing lentiviral plasmids, Dr. Shih-Chieh Lin for providing GFP/Luciferase plasmids, Chen-Ching Liu and James Sze for revising the grammar and scientific writing of the manuscript, the Laboratory Animal Center, College of Medicine, National Cheng Kung University and Taiwan Animal Consortium for the technical support in IVIS, and the Human Biobank, Research Center of Clinical Medicine, National Cheng Kung University Hospital for the technical support of tissue processing. This research was supported by MOST 104-2320-B-006-010-MY2 and MOST 109-2320-B-006-052- from the Ministry of Sciences and Technology of Taiwan, and NCKUH-10904018 from National Cheng Kung University Hospital of Taiwan.

Disclosure of conflict of interest

None.

Abbreviations

GBM, Glioblastoma; SoC, Standard of care; TGF-β, Transforming growth factor-β; Akt, Protein kinase B; CIIR, Consecutive irradiation induced resistance; BK channel, Big conductance calcium-activated potassium channel; BKβ, β subunit of BK channel.

Address correspondence to: Dr. Chun-I Sze, Institute of Basic Medical Sciences, Department of Pathology, National Cheng Kung University Hospital, College of Medicine, National Cheng-Kung University, Tainan 70101, Taiwan. Tel: +886-6-235353-5656; E-mail: szec@mail.ncku.edu.tw; Dr. Po-Wu Gean, Institute of Basic Medical Sciences, Department of Pharmacology, College of Medicine, Department of Biotechnology and Bioindustry Sciences, National Cheng-Kung University, No. 1, Daxue Road, East Dist., Tainan 70101, Taiwan. Tel: +886-6-2353535-5507; E-mail: powu@mail.ncku.edu.tw

References

[1] Weller M and Wick W. Neuro-oncology in 2013: improving outcome in newly diagnosed malignant glioma. Nat Rev Neurol 2014; 10: 68-70.

[2] Louis DN, Perry A, Reifenberger G, von Deimling A, Figarella-Branger D, Cavenee WK, Ohgaki H, Wiestler OD, Kleihues P and Ellison DW. The 2016 world health organization classification of tumors of the central nervous system: a summary. Acta Neuropathol 2016; 131: 803-820.

[3] Johnson DR and O'Neill BP. Glioblastoma survival in the United States before and during the temozolomide era. J Neurooncol 2012; 107: 359-364.

[4] Hein AL, Ouellette MM and Yan Y. Radiation-induced signaling pathways that promote cancer cell survival (review). Int J Oncol 2014; 45: 1813-1819.

[5] van Vulpen M, Kal HB, Taphoorn MJ and El-Sharouni SY. Changes in blood-brain barrier permeability induced by radiotherapy: implications for timing of chemotherapy? (Review). Oncol Rep 2002; 9: 683-688.

[6] Huber SM, Butz L, Stegen B, Klumpp L, Klumpp D and Eckert F. Role of ion channels in ionizing radiation-induced cell death. Biochim Biophys Acta 2015; 1848: 2657-2664.

[7] Willers H, Azzoli CG, Santivasi WL and Xia F. Basic mechanisms of therapeutic resistance to radiation and chemotherapy in lung cancer. Cancer J 2013; 19: 200-207.

[8] Shankar A, Kumar S, Iskander AS, Varma NR, Janic B, deCarvalho A, Mikkelsen T, Frank JA, Ali MM, Knight RA, Brown S and Arbab AS. Subcurative radiation significantly increases cell proliferation, invasion, and migration of primary glioblastoma multiforme in vivo. Chin J Cancer 2014; 33: 148-158.

[9] Osuka S and Van Meir EG. Overcoming therapeutic resistance in glioblastoma: the way forward. J Clin Invest 2017; 127: 415-426.

[10] Abdullaev IF, Rudkouskaya A, Mongin AA and Kuo YH. Calcium-activated potassium channels BK and IK1 are functionally expressed in

human gliomas but do not regulate cell proliferation. PLoS One 2010; 5: e12304.
[11] Bates E. Ion channels in development and cancer. Annu Rev Cell Dev Biol 2015; 31: 231-247.
[12] Rosa P, Sforna L, Carlomagno S, Mangino G, Miscusi M, Pessia M, Franciolini F, Calogero A and Catacuzzeno L. Overexpression of large-conductance calcium-activated potassium channels in human glioblastoma stem-like cells and their role in cell migration. J Cell Physiol 2017; 232: 2478-2488.
[13] Vergara C, Latorre R, Marrion NV and Adelman JP. Calcium-activated potassium channels. Curr Opin Neurobiol 1998; 8: 321-329.
[14] Steinle M, Palme D, Misovic M, Rudner J, Dittmann K, Lukowski R, Ruth P and Huber SM. Ionizing radiation induces migration of glioblastoma cells by activating BK K(+) channels. Radiother Oncol 2011; 101: 122-126.
[15] Stegen B, Butz L, Klumpp L, Zips D, Dittmann K, Ruth P and Huber SM. Ca2+-activated IK K+ channel blockade radiosensitizes glioblastoma cells. Mol Cancer Res 2015; 13: 1283-1295.
[16] Yan L, Xu G, Qiao T, Chen W, Yuan S and Li X. CpG-ODN 7909 increases radiation sensitivity of radiation-resistant human lung adenocarcinoma cell line by overexpression of Toll-like receptor 9. Cancer Biother Radiopharm 2013; 28: 559-564.
[17] Wu SN, Liu SI and Huang MH. Cilostazol, an inhibitor of type 3 phosphodiesterase, stimulates large-conductance, calcium-activated potassium channels in pituitary GH3 cells and pheochromocytoma PC12 cells. Endocrinology 2004; 145: 1175-1184.
[18] Ye YL, Shi WZ, Zhang WP, Wang ML, Zhou Y, Fang SH, Liu LY, Zhang Q, Yu YP and Wei EQ. Cilostazol, a phosphodiesterase 3 inhibitor, protects mice against acute and late ischemic brain injuries. Eur J Pharmacol 2007; 557: 23-31.
[19] Kamparaj SG, Kudagi BL, Muthiah NS, Karikal HP and Pravin KR. Preclinical evaluation of the impact of cilostazol on anti-depressant activity of fluoxetine. International Journal of Research in Pharmaceutical Sciences 2020; 11: 5097-5103.
[20] Kim BM, Hong Y, Lee S, Liu P, Lim JH, Lee YH, Lee TH, Chang KT and Hong Y. Therapeutic implications for overcoming radiation resistance in cancer Therapy. Int J Mol Sci 2015; 16: 26880-26913.
[21] David CJ and Massague J. Contextual determinants of TGFbeta action in development, immunity and cancer. Nat Rev Mol Cell Biol 2018; 19: 419-435.
[22] Drabsch Y and ten Dijke P. TGF-beta signalling and its role in cancer progression and metastasis. Cancer Metastasis Rev 2012; 31: 553-568.
[23] Katsuno Y, Lamouille S and Derynck R. TGF-beta signaling and epithelial-mesenchymal transition in cancer progression. Curr Opin Oncol 2013; 25: 76-84.
[24] Dancea HC, Shareef MM and Ahmed MM. Role of radiation-induced TGF-beta signaling in cancer therapy. Mol Cell Pharmacol 2009; 1: 44-56.
[25] Hardee ME, Marciscano AE, Medina-Ramirez CM, Zagzag D, Narayana A, Lonning SM and Barcellos-Hoff MH. Resistance of glioblastoma-initiating cells to radiation mediated by the tumor microenvironment can be abolished by inhibiting transforming growth factor-beta. Cancer Res 2012; 72: 4119-4129.
[26] Zhang M, Kleber S, Rohrich M, Timke C, Han N, Tuettenberg J, Martin-Villalba A, Debus J, Peschke P, Wirkner U, Lahn M and Huber PE. Blockade of TGF-beta signaling by the TGF-betaR-I kinase inhibitor LY2109761 enhances radiation response and prolongs survival in glioblastoma. Cancer Res 2011; 71: 7155-7167.
[27] Toulany M and Rodemann HP. Phosphatidylinositol 3-kinase/Akt signaling as a key mediator of tumor cell responsiveness to radiation. Semin Cancer Biol 2015; 35: 180-190.
[28] Shamloo B and Usluer S. p21 in cancer research. Cancers (Basel) 2019; 11.
[29] Kim Y, Joo KM, Jin J and Nam DH. Cancer stem cells and their mechanism of chemo-radiation resistance. Int J Stem Cells 2009; 2: 109-114.
[30] Ghatta S, Nimmagadda D, Xu X and O'Rourke ST. Large-conductance, calcium-activated potassium channels: structural and functional implications. Pharmacol Ther 2006; 110: 103-116.
[31] Nishikawa R. Standard therapy for GBM where we are. Neurol Med Chir (Tokyo) 2010; 50: 713-719.
[32] Lau E and Ronai ZA. ATF2 - at the crossroad of nuclear and cytosolic functions. J Cell Sci 2012; 125: 2815-2824.
[33] Li S, Ezhevsky S, Dewing A, Cato MH, Scortegagna M, Bhoumik A, Breitwieser W, Braddock D, Eroshkin A, Qi J, Chen M, Kim JY, Jones S, Jones N, Rickert R and Ronai ZA. Radiation sensitivity and tumor susceptibility in ATM phospho-mutant ATF2 mice. Genes Cancer 2010; 1: 316-330.
[34] Li B, Shi XB, Nori D, Chao CK, Chen AM, Valicenti R and White Rde V. Down-regulation of microRNA 106b is involved in p21-mediated cell cycle arrest in response to radiation in prostate cancer cells. Prostate 2011; 71: 567-574.

[35] Kreis NN, Louwen F and Yuan J. The multifaceted p21 (Cip1/Waf1/CDKN1A) in cell differentiation, migration and cancer therapy. Cancers (Basel) 2019; 11: 1220.
[36] Macleod KF, Sherry N, Hannon G, Beach D, Tokino T, Kinzler K, Vogelstein B and Jacks T. p53-dependent and independent expression of p21 during cell growth, differentiation, and DNA damage. Genes Dev 1995; 9: 935-944.
[37] Stankic M, Pavlovic S, Chin Y, Brogi E, Padua D, Norton L, Massague J and Benezra R. TGF-beta-Id1 signaling opposes Twist1 and promotes metastatic colonization via a mesenchymal-to-epithelial transition. Cell Rep 2013; 5: 1228-1242.
[38] Joseph JV, Balasubramaniyan V, Walenkamp A and Kruyt FA. TGF-beta as a therapeutic target in high grade gliomas - promises and challenges. Biochem Pharmacol 2013; 85: 478-485.
[39] Chang L, Graham PH, Ni J, Hao J, Bucci J, Cozzi PJ and Li Y. Targeting PI3K/Akt/mTOR signaling pathway in the treatment of prostate cancer radioresistance. Crit Rev Oncol Hematol 2015; 96: 507-517.
[40] Kalal BS, Fathima F, Pai VR, Sanjeev G, Krishna CM and Upadhya D. Inhibition of ERK1/2 or AKT activity equally enhances radiation sensitization in B16F10 cells. World J Oncol 2018; 9: 21-28.
[41] Haar CP, Hebbar P, Wallace GC 4th, Das A, Vandergrift WA 3rd, Smith JA, Giglio P, Patel SJ, Ray SK and Banik NL. Drug resistance in glioblastoma: a mini review. Neurochem Res 2012; 37: 1192-1200.
[42] Weaver AK, Bomben VC and Sontheimer H. Expression and function of calcium-activated potassium channels in human glioma cells. Glia 2006; 54: 223-233.
[43] Sizemore G, McLaughlin S, Newman M, Brundage K, Ammer A, Martin K, Pugacheva E, Coad J, Mattes MD and Yu HG. Opening large-conductance potassium channels selectively induced cell death of triple-negative breast cancer. BMC Cancer 2020; 20: 595.
[44] Ge L, Hoa NT, Wilson Z, Arismendi-Morillo G, Kong XT, Tajhya RB, Beeton C and Jadus MR. Big Potassium (BK) ion channels in biology, disease and possible targets for cancer immunotherapy. Int Immunopharmacol 2014; 22: 427-443.
[45] Pardo LA and Stuhmer W. The roles of K(+) channels in cancer. Nat Rev Cancer 2014; 14: 39-48.
[46] Edalat L, Stegen B, Klumpp L, Haehl E, Schilbach K, Lukowski R, Kuhnle M, Bernhardt G, Buschauer A, Zips D, Ruth P and Huber SM. BK K+ channel blockade inhibits radiation-induced migration/brain infiltration of glioblastoma cells. Oncotarget 2016; 7: 14259-14278.
[47] McManus OB, Helms LM, Pallanck L, Ganetzky B, Swanson R and Leonard RJ. Functional role of the beta subunit of high conductance calcium-activated potassium channels. Neuron 1995; 14: 645-650.
[48] Chen L, Bi D, Lu ZH, McClafferty H and Shipston MJ. Distinct domains of the beta1-subunit cytosolic N terminus control surface expression and functional properties of large-conductance calcium-activated potassium (BK) channels. J Biol Chem 2017; 292: 8694-8704.
[49] Kraft R, Krause P, Jung S, Basrai D, Liebmann L, Bolz J and Patt S. BK channel openers inhibit migration of human glioma cells. Pflugers Arch 2003; 446: 248-255.
[50] Huang X and Jan LY. Targeting potassium channels in cancer. J Cell Biol 2014; 206: 151-162.
[51] Turner KL and Sontheimer H. Cl- and K+ channels and their role in primary brain tumour biology. Philos Trans R Soc Lond B Biol Sci 2014; 369: 20130095.
[52] Gueguinou M, Chantome A, Fromont G, Bougnoux P, Vandier C and Potier-Cartereau M. KCa and Ca(2+) channels: the complex thought. Biochim Biophys Acta 2014; 1843: 2322-2333.
[53] Rosa P, Catacuzzeno L, Sforna L, Mangino G, Carlomagno S, Mincione G, Petrozza V, Ragona G, Franciolini F and Calogero A. BK channels blockage inhibits hypoxia-induced migration and chemoresistance to cisplatin in human glioblastoma cells. J Cell Physiol 2018; 233: 6866-6877.
[54] Samuel P, Pink RC, Caley DP, Currie JM, Brooks SA and Carter DR. Over-expression of miR-31 or loss of KCNMA1 leads to increased cisplatin resistance in ovarian cancer cells. Tumour Biol 2016; 37: 2565-2573.
[55] Vander Heiden MG, Cantley LC and Thompson CB. Understanding the Warburg effect: the metabolic requirements of cell proliferation. Science 2009; 324: 1029-1033.
[56] Burns JS and Manda G. Metabolic pathways of the warburg effect in health and disease: perspectives of choice, chain or chance. Int J Mol Sci 2017; 18: 2755.
[57] Hockel M and Vaupel P. Tumor hypoxia: definitions and current clinical, biologic, and molecular aspects. J Natl Cancer Inst 2001; 93: 266-276.
[58] Zhou Y, Xia XM and Lingle CJ. BK channel inhibition by strong extracellular acidification. Elife 2018; 7: e38060.
[59] Xing F, Luan Y, Cai J, Wu S, Mai J, Gu J, Zhang H, Li K, Lin Y, Xiao X, Liang J, Li Y, Chen W, Tan Y, Sheng L, Lu B, Lu W, Gao M, Qiu P, Su X, Yin W, Hu J, Chen Z, Sai K, Wang J, Chen F, Chen Y, Zhu S, Liu D, Cheng S, Xie Z, Zhu W and Yan G.

The anti-warburg effect elicited by the cAMP-PGC1alpha Pathway drives differentiation of glioblastoma cells into astrocytes. Cell Rep 2017; 18: 468-481.

[60] Tanano I, Nagaoka T, Omae T, Ishibazawa A, Kamiya T, Ono S and Yoshida A. Dilation of porcine retinal arterioles to cilostazol: roles of eNOS phosphorylation via cAMP/protein kinase A and AMP-activated protein kinase and potassium channels. Invest Ophthalmol Vis Sci 2013; 54: 1443-1449.

[61] Li H, Hong DH, Son YK, Na SH, Jung WK, Bae YM, Seo EY, Kim SJ, Choi IW and Park WS. Cilostazol induces vasodilation through the activation of Ca(2+)-activated K(+) channels in aortic smooth muscle. Vascul Pharmacol 2015; 70: 15-22.